Available online at www.sciencedirect.com
ScienceDirect
Journal of Nuclear Materials 363–365 (2007) 649–657
journal of nuclear materials
www.elsevier.com/locate/jnucmat

Detailed atomic, molecular and radiation kinetics in current 2D and 3D edge plasma fluid codes

D. Reiter [a,*], V. Kotov [a], P. Börner [a], K. Sawada [b], R.K. Janev [a], B. Küppers [a]

[a] *Institut für Plasmaphysik, Forschungszentrum Jülich GmbH, EURATOM-Association, Trilateral Euregio Cluster, D-52425 Jülich, Germany*
[b] *Department of Applied Physics, Faculty of Engineering, Shinshu University, Nagano 380-8553, Japan*

Abstract

Predictive and interpretative edge plasma models often rely upon a kinetic neutral particle module. A virtually exact description of atomic, molecular and radiative reactions is provided via Monte Carlo synthesis of the relevant processes. For many integrated edge transport models, such as *B2–EIRENE* ('*SOLPS*'), *OEDGE*, *EDGE2D–EIRENE* (all 2D) and *EMC3–EIRENE* (3D) the EIRENE Monte Carlo code provides this microscopic analysis for the macroscopic plasma flow fields. The current status of the neutral-particle and radiation transport model in the EIRENE Monte Carlo Code is presented. The directions of further developments of the databases are outlined.

PACS: 51.10.+y; 52.25.Jm; 52.25.Ya; 52.25.Os

Keywords: Divertor modelling; EIRENE; Hydrocarbon; Photon transport

1. Introduction

In a number of recent applications of the EIRENE neutral particle transport and radiation transfer code [1] reference is made to upgraded atomic and molecular packages, both in stand alone applications, [2], interpretative mode of operation, e.g. [3,4], or predictive applications [5]. Significant differences have been reported for ITER predictions, due to these upgrades [6]. These have, for example, re-initiated the consideration of the ITER dome removal issue [5,7].

In this paper the current status in these extensions of the atomic, molecular and radiative model is made explicit, the level of approximation still present in the code, and the currently newly compiled databases are analyzed with respect to involved timescales (stiffness). In particular the concept of radiation stimulated ionization (RSI) (and associated electron cooling) is introduced, which allows a self consistent, multi-line and non-LTE neutral gas and radiation transport Monte Carlo simulation with only minimal modifications to the existing EIRENE code and databases.

Recently the EIRENE options for neutral–neutral collisions (i.e., viscosity, friction and heat conduction

* Corresponding author.
E-mail address: d.reiter@fz-juelich.de (D. Reiter).
URL: http://www.eirene.de (D. Reiter).

0022-3115/$ - see front matter © 2007 Elsevier B.V. All rights reserved.
doi:10.1016/j.jnucmat.2007.01.213

effects within the neutral component) [8] have been activated in coupled B2–EIRENE calculations. Some brief comments are given here on this as well.

1.1. Recent applications of EIRENE to ITER and Alcator C-Mod

The role of atomic and molecular collision kinetics on divertor plasma dynamics can be expected to be largest in the detached regime, in which not only re-ionization and cooling, but also recombination and friction between plasma and gas are relevant. The divertor collisionality (size R times density n_e) in JET is about 10–15 times smaller than in ITER, Alcator C-Mod is still a factor 6–7 away but is the divertor experiment closest to ITER in this parameter which is currently available. In [2] a comprehensive assessment of atomic and molecular effects has been given for this machine, using an extensive set of experimental data. In particular it was shown that radiation transfer (trapping of the resonance Lyman lines) becomes significant. The results in [2] have been obtained with account for trapping effects for the Ly_α line alone, and with Doppler (and natural) broadening as the only line broadening mechanism. In the meantime the radiation transfer module of the EIRENE code has been further upgraded, now including multiple lines, the normal Zeeman triplet, a full Zeeman–Stark line shape code for the Ly_α line and a consistent coupling to the 2D B2 and EDGE2D and the 3D EMC3 edge plasma fluid transport codes. Fig. 1 shows the ionization distribution in Alcator C-Mod for the same discharge conditions as investigated in [2], once from the conventionally collisional radiative model for hydrogen atoms, and once the additional contribution initiated by radiation trapping (radiative stimulated ionization: RSI). These ionization processes are additive and missing in neutral gas simulations invoking the optically thin approximation. They account for about 30% of the total ionization rate in this discharge. Of these 30% extra ionization 77% proceeds through Ly_α reabsorption, 18% via Ly_β, 4% via Ly_γ and the rest through higher states. The refined model confirms, even quantitatively the earlier speculations in [2]. The somewhat reduced opacity due to the added (normal) Zeeman line splitting in the strong magnetic field (6–7 T in the relevant region) is compensated by additional opacity of the Ly_β and (very weakly) also the Ly_γ lines now added. As found before the neutral gas density in the divertor drops by about a factor 1.8 if opacity

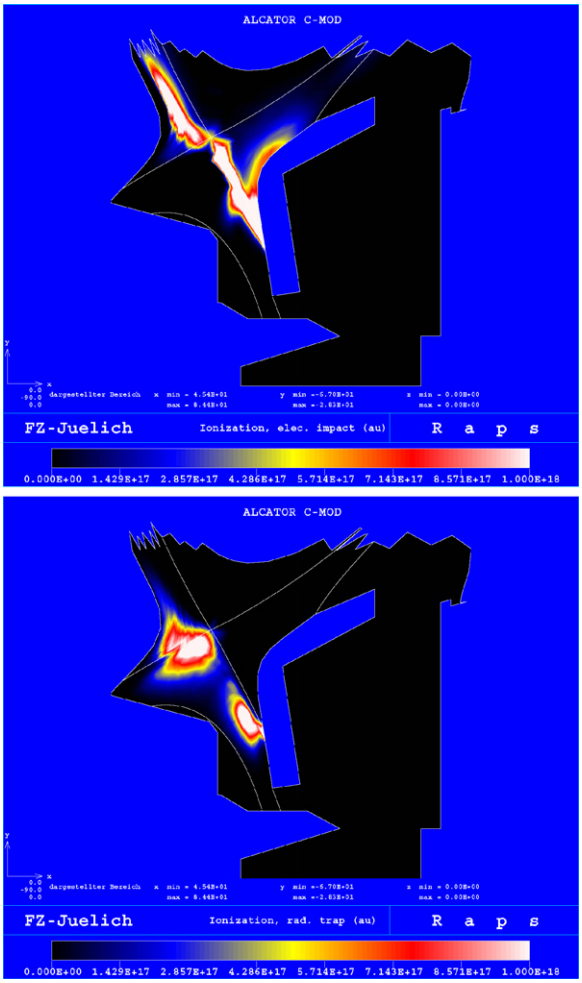

Fig. 1. Ordinary (top) and photon stimulated (RSI) (bottom) ionization in Alcator C-Mod divertor, plasma conditions from Ref. [2]. The same linear colour shading code is used for the rates in both figures. The reader is referred to the web version of this article for this colour code.

effects are accounted for, on a fixed measured plasma background.

The ITER applications [5,6] differ from those for C-Mod in that here the plasma state is allowed to respond, in a self-consistent way, to radiation trapping and the other model refinements. The most relevant engineering divertor parameter (pumping plenum gas pressure vs. peak target heat flux) are found to be quite insensitive to the way in which re-ionization occurs, although the divertor state now is characterized by a higher plasma density (up to a factor 2, locally), reduced electron temperature and a significant shift from target recycling towards volume recombination as charge sink. Radiation of the dominant Ly_α line is almost 100% trapped, and

60–90% of the ionization in the inner divertor occurs via the additional RSI route (loc.cit.). Despite this the radiative heat transfer, e.g. into the private flux region, is very small, as can be seen from the only weakly affected T_e profiles after adding electron energy gain/loss rates due to RSI, see Fig. 2. This is due to the very short photon mean free pathes in ITER. A similar assessment, for Alcator C-Mod conditions with a coupled plasma-neutral-radiation code might still support the possibility of a radiatively sustained PFR. A summary of effects from refined atomic and molecular kinetics, on peak target heat flux vs. plenum pressure for ITER, is shown in Fig. 3.

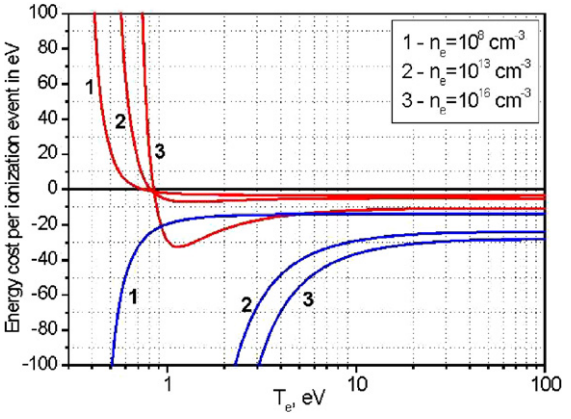

Fig. 2. Energy cost or gain per ionization, for ordinary (blue) and photon stimulated ionization (RSI), red. Comparing with Fig. 1 suggests the possibility of radiative heat transfer into PFZ. (For interpretation of the references in colour in this figure legend, the reader is referred to the web version of this article.)

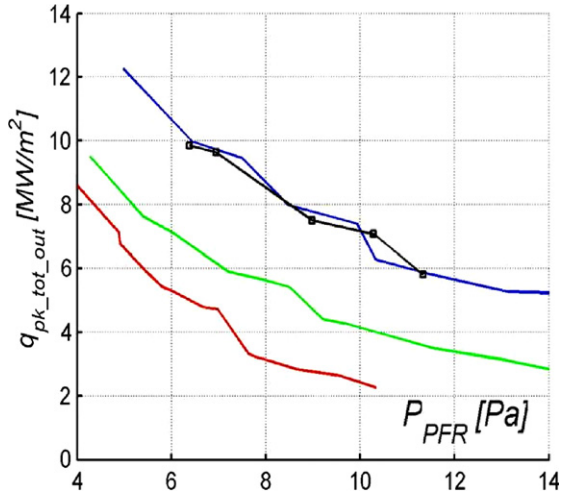

Fig. 3. ITER scaling of peak target heat load vs. divertor plenum gas pressure. Lowest curve: original scaling (EIRENE 1996 as in previous SOLPS), middle curve: neutral neutral collision included, upper curve: refined molecule collision kinetics (see text). Black curve on top of upper curve: radiation trapping included.

2. Detailed atomic, molecular and radiation kinetics

Despite major upgrades in the past years, there is still a number of approximations involved in present EIRENE applications. These are due to either the 'historical' choice of input parameters, or due to code restrictions. We discuss them by resorting to the equations that are solved by EIRENE.

EIRENE has implemented conventional Monte Carlo methods for solving linear Boltzmann equations for the distribution function in phase space f [1]. For a mixture of neutral particles (species labelled by i) this results in a coupled system

$$\left[\frac{\partial}{\partial t}+\mathbf{v}\cdot\nabla\right]f_i(\mathbf{r},\mathbf{v},t)+a_{ii}(\mathbf{r},\mathbf{v},t)f_i(\mathbf{r},\mathbf{v},t) = S_i(\mathbf{r},\mathbf{v},t)+\sum\nolimits_j\int d^3v' C_{ij}(\mathbf{v}'\rightarrow\mathbf{v})f_j(\mathbf{r},\mathbf{v}',t). \quad (1)$$

Here a_{ii} is the extinction coefficient, S_i the external source rate for species i (recycling, volume recombination, gas puff, etc.), and the operator C_{ij} describes collision processes (particles emerging from collisions).

In this linear set of equations non-linear processes (e.g. elastic neutral–neutral collisions) are treated in BGK approximation, either by internal iterations within a single EIRENE run [8], or, in cases with coupling to external plasma transport codes such as B2 or EMC3, via the neutral-plasma-iterations. Macroscopic neutral gas parameters, such as density, kinetic temperature, flow velocity, found in one iteration are used for specifying artificial neutral background species b (together with the host medium consisting of electrons and fluid-ions). In the next iteration the neutral particle solution is calculated including also (self-)collisions with these background neutrals from the previous iteration. Collision times for the BGK collision term are input parameters. For self and cross collisions between neutral species they are derived from (experimental) gas viscosity and binary diffusion coefficients and they depend weakly on gas temperature (loc.cit.). Convergence is monitored via decrease of residual changes in the macroscopic gas parameters between iterations [6,7].

The radiation transport equation for the spectral intensity I_i from a particular transition i is solved by EIRENE in a way completely analogous to the

particle transport equation (after transformation of velocity space coordinates into frequency or energy E and direction $\mathbf{\Omega}$)

$$\left[\frac{1}{c}\frac{\partial}{\partial t}+\mathbf{\Omega}\cdot\nabla\right]I_i(\mathbf{r},\mathbf{\Omega},E,t) + a_{ii}(\mathbf{r},\mathbf{\Omega},E,t)I_i(\mathbf{r},\mathbf{\Omega},E,t)=S_i(\mathbf{r},\mathbf{\Omega},E,t) + \sum_j\int_0^\infty \mathrm{d}E'\oint \mathrm{d}\mathbf{\Omega}' R_{ij}(E'\to E,\mathbf{\Omega}'\cdot\mathbf{\Omega})I_j(\mathbf{r},\mathbf{\Omega}',E',t). \tag{2}$$

The non-linear radiation absorption is dealt with by a similar iterative scheme as neutral–neutral collisions, using macroscopic neutral gas parameters from a previous iteration to formulate a background medium for absorption of line radiation, and line absorption rates from a previous photon iteration are used for computing the additional RSI rate coefficients for neutrals. Note that the radiative and three-body recombination rates are not affected by radiation trapping, as can be seen from the CR model equations for this coupled kinetic system [6].

Comparing Eq. (1) with this equation one easily sees that Eq. (2) is, actually, nothing but a strangely normalized Boltzmann equation for photons. For convenience the spectrum is split in EIRENE into individual lines (e.g. $i=1$: Ly_α, $i=2$: Ly_β) which are also labelled by an index i. Multi-line transport is thus carried out in a way analogous to the multi-species gas transport, and also line-mixing is included via the scattering operator ('redistribution function') R_{ij}.

The scattering operator C_{ij} is given in terms of microscopic differential cross sections $\sigma_{ij}(v_{\mathrm{rel}},\theta)$ for the various collision processes, v_{rel},θ denoting the relative velocity of collision partners and θ the scattering angle, respectively. We write $C_{ij}=n_b\langle\sigma^t_{ij}v_{\mathrm{rel}}\rangle g(\mathbf{v}_j\to\mathbf{v}_i)$, with the brackets denoting averaging of the total cross section $\sigma^t_{ij}(v_{\mathrm{rel}})$ over a drifting Maxwellian background (electrons, ions, but also neutrals from the previous iteration). n_{b} is the background particle density. g is the probability of finding particle species i with velocity $\mathbf{v}_i$, given a particle of species j and velocity $\mathbf{v}_j$ has collided with host medium particle of type b.

Similarly the kernel R_{ij} can be written as product of a rate r and a normalized redistribution function $h_{ij}(E,\mathbf{\Omega}\to E,\mathbf{\Omega})$.The rate r is given by the Einstein coefficients A_{ij}, B_{ij} or B_{ji}, transformed to proper units.

Cross sections, rate coefficients and optical parameters of the individual lines (photon species) are read from external databases. The following approximations are still made in EIRENE:

(1) For all electron impact collisions $v_{\mathrm{rel}}=v_{\mathrm{e}}$, the electron velocity. A very well justified approximation.
(2) For all dissociative electron impact collisions the post collision heavy particle velocity distribution is independent of incident velocity $\mathbf{v}'$ in the center of mass frame, isotropic, with a constant kinetic energy release ΔE_{kin} (input, together with the cross section) shared amongst products inversely proportionally to their masses. For two post collision products (dissociation) this follows from momentum conservation, for three or more products this is not motivated by anything other than lack of knowledge. In particular the assumption of a constant value ΔE_{kin} per reaction is questionable. For H_2, H_2^+ dissociation recently far more detailed distributions, based upon potential curves and the Franck–Condon overlap principle, have been derived and coded by one of us (K. Sawada). They have not yet been implemented into EIRENE.
(3) For charge exchange the scattering angle dependence in the differential cross section is assumed to be a delta function at $\theta=\pi$, this expressing exchange of identity. For resonant charge exchange (e.g. H + p) this choice already accounts for the 'true' elastic component, which hence must NOT be added on top of that.
(4) Although EIRENE can also handle differential cross sections e.g. from quantal calculations, elastic collisions between charged particles and neutrals are simulated by following the classical orbits of collision partners in generalized Morse like potential [9]. We are not aware of a detailed comparison which shows that this approximation is critical. The $p+H_2$ elastic collision process has been found to be a most important player in detached divertor plasma conditions for ITER, JET and Alcator C-Mod, see again Fig. 3 and [2,6]. It is available in EIRENE since 1992, but has been hardly ever activated before the 2003 revisions of the ITER edge codes and the OSM–EIRENE applications for Alcator C-Mod.
(5) For photons one very common but perhaps critical assumption made is that of so called 'complete redistribution' in the function h_{ij}.

It means that prompt re-emission as photon of line i after the absorption of a photon of line j is treated as independent from frequency and direction of the absorbed photon. This eliminates the scattering kernel R_{ij} from the radiation transport equation, because this part can then be condensed into the source function S_i, i.e. be combined with the contribution of emission after excitation by electron impact. This very common approximation is strictly valid only under high enough densities. Its validity for divertor plasma conditions has, to our knowledge, not yet been investigated. Note that this approximation does not eliminate options for treating line mixing: the extinction coefficient a_{ii} is obtained from the sum over all processes for photons of line i, i.e., also possibly from absorption of a photon of line i by a transition with line shape h_{ji} belonging to another line j, if these overlap sufficiently, e.g. due to Doppler broadening. This effect still has to be studied in ITER applications, in case of DT mixtures. Depending upon gas temperature the Lyman lines for D and T can be partially or even fully separated. Hence the present model without separating these species may somewhat overestimate the opacity effect for D–T plasmas, see Fig. 4.

The line shapes used in ITER and DEMO applications [5] and other recent applications have been Doppler broadened normal Zeeman triplets.

EIRENE has very recently been equipped with an additional anisotropic line shape $h_{ii}(E,\mathbf{\Omega})$ for the Ly_α transition obtained with the PPP code (see J. Rosato, this proceedings). $\mathbf{\Omega}$ is the angle of emission (or at absorption) against the B-field. This line shape includes the full Zeeman (fine-structure) splitting, electron and ion Stark broadening as well as the motional Stark effect. For implementation into EIRENE $h_{ii}(E,\mathbf{\Omega})$ is written as $h1(\mathbf{\Omega})h2_{ii}(E|\mathbf{\Omega})$. $h1$ is the isotropic distribution of the angle, and $h2$ is the frequency distribution for a given angle. $h2$ is given as weighted sum of 10 Lorentzian profiles from which E can directly be sampled by inversion, and also the Doppler convolution (for the line absorption coefficient) is given analytically, then as weighted sum of 10 Voigt functions. Fig. 5 proves the correct implementation by comparing the random sampling from $h2$ (for emission) with the analytically convoluted line shape for absorption. It also shows that due to the dominance of the Doppler effect the earlier calculations using simpler line shapes have probably been already sufficiently accurate.

(6) The species index i in Eq. (1) labels atoms, molecules, their ions, selected for a particular case and their excited states (both electronically and vibrationally). A crucial approximation is formal ordering of the second term on the left side in this equation, the absorption term, with $1/\epsilon$, ϵ a smallness parameter. Then the first term on the left, the convection term is neglected as compared to this very large term. In EIRENE this choice can now be made for all species individually, hence automatically constructing kinetic collisional radiative approximations. The species in the group with this neglected convection term are treated in quasi steady state (QSS), i.e., they stick to their place of birth and only the collision kernel is sampled until a species is created which does not belong to this QSS group of species. Then the ordinary Monte Carlo particle tracing resumes.

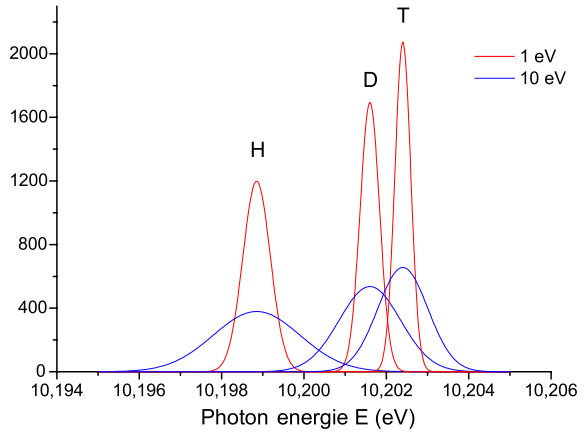

Fig. 4. Doppler broadened Lyman alpha line shapes from H, D, T for 1 and for 10 eV gas temperature, resp., showing clear line separation at 1 eV.

In all EIRENE applications until now this choice has always been made for H_2^+ ions formed by dissociation from H_2. It would, of course, be patently foolish to use this Monte Carlo QSS approximation

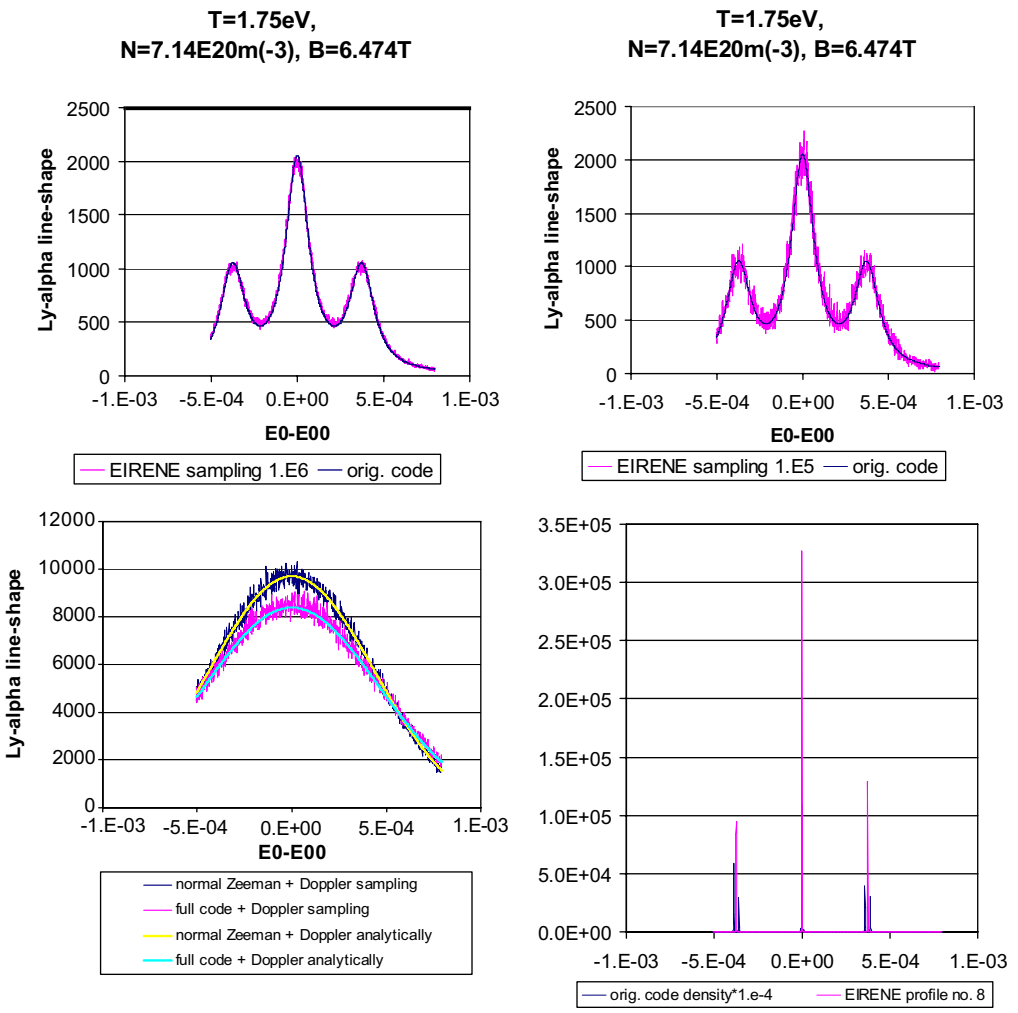

Fig. 5. Comparison of sampled and analytically evaluated Zeeman–Stark line shape, normal to B-field. For $B = 6$ T, $T_e = T_i = 1.75$ eV, $n = 6e20$, top left: 1e6 samples, top right: 1e5 samples. Bottom left: additional Doppler broadening, T-gas = 1.75 eV, comparison new PPP code line shape with previous normal Zeeman + Doppler profile. Bottom right: PPP line shape, with n reduced by 1e4 and no Doppler broadening. Fine structure becomes visible.

to eliminate very fast (radiative decay) processes from the system. For electronic and vibrationally excited states of H, H_2, He and C pre-computed solutions to the QSS equations with neglected heavy particle collision terms (charge exchange, elastic collisions) are available on EIRENE databases, vs. electron density and temperature, as so called effective CR-ionization, dissociation and recombination rates.

Activation of these for H_2 transport, rather than using single step ionization and dissociation rate coefficients, together with activation of the $p + H_2(v) \rightarrow H + H_2^+$ ion conversion is the 'refined molecule collision kinetics' referred to in ITER applications since 2004. Missing in this model are still the accompanying refined electron energy losses, which are still assumed to be constant for H_2 (as in older models), and the post collision kinetic energy distributions, see point (2), above. Apart from vibrationally excited $H_2(v)$ molecules, these QSS assumptions are believed to be highly accurate. For $H_2(v)$ until now no significant differences on macroscopic divertor parameters due to evoking this approximation in EIRENE compared to full cases have been observed. The same holds true for He, in which the two meta-stable triplet states can either be fully treated or in QSS approximation. In all ITER and other SOLPS applications the QSS approximation for meta-stable He states and $H_2(v)$ has been used throughout.

3. Hydrocarbon catabolism, the HYDKIN online tool

With respect to Hydrocarbon transport in divertors still crude assumptions are typically made in integrated edge modelling, usually neglecting the breakup-chain altogether and treating only the final C atoms. Earlier databases used to model hydrocarbon chemistry in fusion plasmas are either entirely obsolete or largely empirical [10]. The most recent cross section compilations [11,12] now provide an up to date database, up to propane, C_3H_8, based on most recent experimental and theoretical data, on thermochemical data and on physically motivated cross section scaling relationships.

The required chemical complexity in a model is determined by the relevant chemical timescales. In order to be able to assess these for any individual case, the cross section database and the integration into Maxwellian rate coefficients is provided online by the HYDKIN code (see URL in [1]). Electron impact cross sections are integrated into Maxwellian rate coefficients (vs. T_e). In case of charge exchange and particle rearrangement collisions the rate coefficients are given as function of fixed energy E of the C_xH_y particle and the temperature T_p of the protons. From these a straightforward scaling to double (drifting) Maxwellian averages, even with differing temperatures and relative drift velocities of the reactants, is readily possible.

The HYDKIN tool also provides the online solution of the QSS model. It is initiated by selecting the chemical species amongst the hydrocarbons to be included in the analysis, the parameters of the constant reservoir (background medium) (electrons and hydrogenic ions, by default). The master equation describing the reaction kinetics $d\vec{Y}/dt = \mathbf{A}\vec{Y} + \vec{b}$ is automatically build from the database. This master equation follows directly from Eq. (1) by integrating over velocity space, assuming homogeneous conditions and a constant energy E of hydrocarbons. $\vec{Y}$ denotes the vector of selected species concentrations (e.g. [particles or mols per unit volume], $\mathbf{A}$ is the master operator matrix with elements a_{ij} being the rates of conversion from species j to i, (compare to C_{ij}) and, optionally $\vec{b}$ (compare to S_i) is the vector of influx of the selected species from an external reservoir. Any particular reaction from the present databases can be written as $1R + s_1Y_1 \rightarrow r_rR + r_1Y_1 + r_2Y_2 + r_3Y_3 \ldots$. Here s_i and r_j are the stoichiometric coefficients, R is the concentration of a species from the reservoir (i.e., an electron in case of I-DI, DE, DI^+, DE^+ and DRC processes or a hydrogen ion for CX and PR processes, [11,12]). The diagonal elements of $\mathbf{A}$ read: $a_{ii} = -Y_i/\tau_{\mathrm{loss},i} - \sum_j a_{ij}$ with $\tau_{\mathrm{loss},i}$ denoting the loss time of species i from the system (e.g. to walls or due to outflow). After specification of the vectors $\vec{b}, \vec{\tau}$ and $\vec{Y}(t=0)$, the initial condition, the solution $\vec{Y}(t)$ is found by expansion in eigenfunctions $\vec{Y}(t) = \sum_i c_i\vec{\Psi}_i$ with $\vec{\Psi}_i = \vec{\xi}_i \exp(\lambda_i t)$, λ_i and $\vec{\xi}_i$ denoting the ith eigenvalue and eigenvector respectively, and the c_i are constants to be determined from the initial condition. For zero influx $\vec{b}$ and loss $\vec{Y}_{\mathrm{loss}}$ the final absorbing species span the kernel of $\mathbf{A}$ (i.e., they are determined by the eigenvectors for eigenvalue zero). All other selected species are transient. In case of influx from an external reservoir: $\vec{b} \neq 0$ and still $\vec{Y}_{\mathrm{loss}} = 0$, e.g. due to chemical sputtering or an external gas puff of some C_xH_y, the concentrations of these final species are linearly increasing with time t.

This linear master equation describes on open system, because electron and proton densities are kept at constant values. Due to the particular choice of processes in [11,12] the matrix $\mathbf{A}$ is upper triagonal and, hence, has only real eigenvalues, which are given by the elements in the diagonal a_{ii}, i.e., by the extinction coefficients for each species. If radiative or three-body (non-dissociative) recombination processes are added (one of the planned further upgrades of the database), then the matrix $\mathbf{A}$ will take Hessenberg form. After the solution is found, also an online evaluation of photon efficiencies for divertor spectroscopy D/XB is carried out, i.e., vs. T_e, T_p, energy E of hydrocarbons, database choice and influx and loss rate composition, for a number of CH and C_2 molecular bands.

Fig. 6, top, shows, vs. plasma temperature (here for: $T_e = T_p$), the ratio of fastest to slowest timescale ('stiffness parameter') in hydrocarbon catabolism in hydrogen plasmas (these ratios are density independent, as long as non-dissociative recombination of hydrocarbons is not included, as it is the case until now). One sees that, except for the low (below 2–3 eV) temperature region no separation of timescales in the reaction dynamics is involved, for any of the primary hydrocarbons released from divertor surfaces (shown here: for CH_4, C_2H_6 and C_3H_8. If one restricts the range of timescales to 100, one can see from Fig. 6, bottom, that still the full set of species (e.g. 48 in case of C_3H_8) has to be kept in the transport simulations. Only below 2–3 eV can a reduced model (with 3–5 'species' (eigenmodes) to be retained) be justified on this basis.

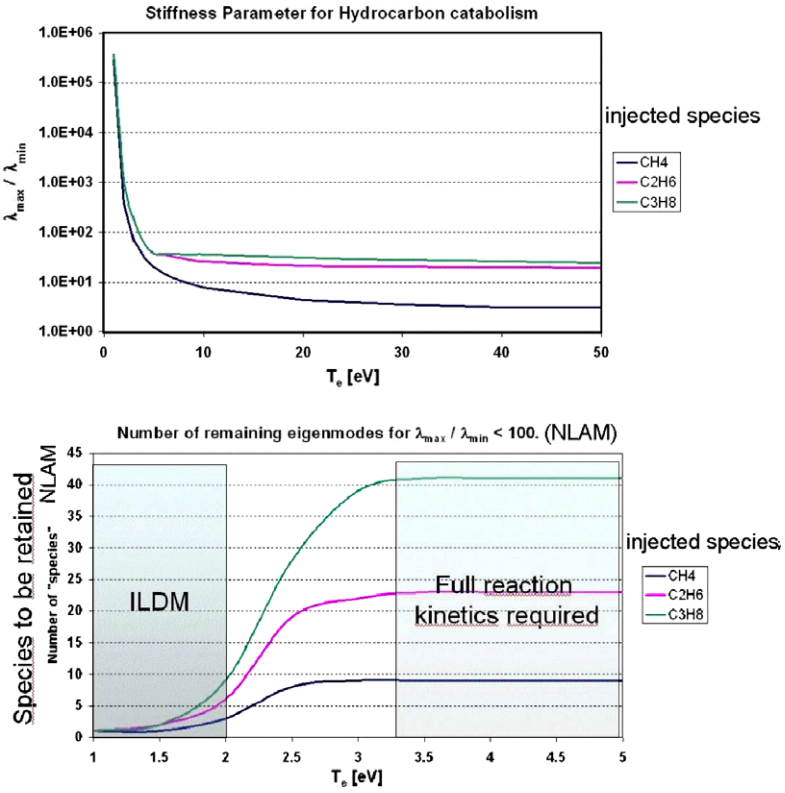

Fig. 6. Top: ratio of largest to smallest timescale in Hydrocarbon catabolism, vs. T_e for incident methane, ethane and propane. Bottom: number of remaining eigenmodes after eliminating all modes with timescales 100 times faster than the slowest, indicating the possibility of accurate simplified models only at T_e less than 3 eV.

4. Conclusions

A number of the more advanced EIRENE options typically absent in SOLPS (B2–EIRENE) setups, such as neutral–neutral collisions and radiation transfer, have recently been activated in the B2–EIRENE code used for ITER divertor modelling. These upgrades exclusively consist of further classical effects which are known be operative under such conditions. Neutral–neutral collisions are still based on the EIRENE multi-species BGK relaxation ansatz and its limited accuracy (Prantl number of one, rather than the correct value 2/3), has to be kept in mind when going to even larger machines (DEMO), in which these processes will become even more relevant. The radiation transport has been completed by adding anisotropic Zeeman splitted (normal Zeeman effect) line shapes as well as, very recently, for the most important Ly_α line, the full (fine structure) Zeeman–Stark profiles (impact approximation for both electrons and ions). Depending on conditions, about 60–90% of ionization in ITER proceeds via radiative excitation, for Alcator C-Mod these are about 30% and for JET still 10–20%, with significant consequences for model comparisons or predictions with the conventional models in which resonance radiation is regarded as optically thin. Major progress has been achieved with respect to processing and analyzing the most recent databases for Hydrocarbon catabolism. A spectral analysis of these databases indicates the possibility of reduced but still accurate models only at low plasma temperatures (below 3 eV), whereas above these temperatures simplifications cannot be justified on the basis of timescales.

References

[1] D. Reiter et al., Fus. Sci. Technol. 47 (2005) 172. http://www.eirene.de/.
[2] S. Lisgo, P. Börner, C. Boswell, et al., J. Nucl. Mater. 337–339 (2005) 139.
[3] S. Brezinsek et al., J. Nucl. Mater., these Proceedings, doi:10.1016/j.jnucmat.2007.01.190;
P. Stangeby et al., J. Nucl. Mater., these Proceedings, doi:10.1016/j.jnucmat.2007.01.008;
D. Elder et al., J. Nucl. Mater., these Proceedings, doi:10.1016/j.jnucmat.2007.01.004.

[4] F. Sardei et al., J. Nucl. Mater., these Proceedings, doi:10.1016/j.jnucmat.2006.12.068;
Y. Feng et al., J. Nucl. Mater., these Proceedings, doi:10.1016/j.jnucmat.2007.01.122;
M. Kobayashi et al., J. Nucl. Mater., these Proceedings, doi:10.1016/j.jnucmat.2007.01.038.
[5] M. Baeva et al., J. Nucl. Mater., these Proceedings, doi:10.1016/j.jnucmat.2007.01.029;
A. Kukushkin et al., J. Nucl. Mater., these Proceedings, doi:10.1016/j.jnucmat.2007.01.094.
[6] V. Kotov, D. Reiter, A. Kukushkin, et al., Contrib. Plasma Phys. 46 (7–9) (2006) 635;
A.S. Kukushkin et al., Nucl. Fus. 45 (2005) 608.
[7] A.S. Kukushkin, H.D. Pacher, V. Kotov, et al., in: 32nd EPS Conference on Plasma Phys. Tarragona, 27 June–1 July 2005 ECA, vol. 29C, P-1.025, 2005.
[8] D. Reiter, C. May, M. Baelmans, et al., J. Nucl. Mater. 241–243 (1997) 342.
[9] D. Reiter, P. Bachmann, A.K. Prinja, Contr. Plasma Phys. 32 (3/4) (1992) 261.
[10] A.B. Ehrhardt, W.D. Langer, Report PPPL-2477, Princeton Plasma Physics Laboratory, Princeton USA, 1987.
[11] R.K. Janev, D. Reiter, Phys. Plasmas 9 (2002) 4071.
[12] R.K. Janev, D. Reiter, Phys. Plasmas 11 (2004) 780.